DOMAIN-SPECIFIC DIFFERENCES BETWEEN ALPHA- AND BETA-SYNUCLEIN SERVE AS A THRESHOLD FOR FIBRIL FORMATION IN COMBINATION WITH CHANGES IN ENVIRONMENTAL CONDITIONS

By

MICHAEL P. OLSON

A thesis submitted to the

Graduate School-New Brunswick

Rutgers, The State University of New Jersey

In partial fulfillment of the requirements

For the degree of

Master of Science

Graduate Program in Chemistry and Chemical Biology

Written under the direction of

Jean Baum and Sagar Khare

And approved by

_____

_____

_____

New Brunswick, New Jersey

October, 2016

ABSTRACT OF THE THESIS

Domain-specific differences between alpha- and beta-synuclein serve as a threshold for fibril formation in combination with changes in environmental conditions

by MICHAEL P. OLSON

Thesis Directors:

Jean Baum and Sagar Khare

Alpha-synuclein (asyn) is a 140 amino acid intrinsically disordered protein that is known to form fibrils found in patients with Parkinson's Disease and Dementia with Lewy Bodies. Beta-synuclein (bsyn) is a homolog of asyn, but is not known to form fibrils and is an inhibitor of asyn aggregation under physiological conditions. Both proteins can be divided into three domains with distinct properties: N-terminal, NAC, and C-terminal. By combining domains of asyn and bsyn to form chimera structures and analyzing them through a combination of Thioflavin T binding assays, NMR, AFM, and computational studies of each expected fibril state, this study will show that chimeras with a bsyn NAC region require a reduction in pH to form fibrils, while asyn NAC chimeras are more similar to asyn in their aggregation behavior and possibly energetics within the fibril state. The regions flanking the NAC seemed to be able to regulate aggregation, where certain combinations were more inhibiting of aggregation (asyn N-terminal with bsyn C-terminal), while one combination may have actually accelerated

aggregation (bsyn N-terminal with asyn C-terminal) relative to asyn. Computational studies made clear that the bsyn NAC proteins must have a different fibrillar structure than asyn, and a combination of NMR chemical shift data and energies determined from computation supported the idea that some allosteric effects may influence a possibly crucial region in the chimeras (residues ~55 to 60). This study provided more information as to how a protein like bsyn can possibly overcome the influence of inhibiting regions under non-physiological conditions to form fibrils and indicates that utilizing the properties of bsyn's C-terminal domain can lead to the proposal of especially effective inhibitors of asyn aggregation.

Acknowledgements

I would especially like to thank current Baum lab member Gina Moriarty for making significant contributions in sharing ideas, assistance with data processing, creating figures, and planning each of the experiments described here as well as performing experimental work related to this thesis. Her ideas and recommendations allowed this work to proceed. I would like to thank former lab member Dr. Maria Janowska, who contributed significantly to the ideas needed to perform this work and provided significant help with making plots of chemical shift differences in R. I would also like to thank current lab member Tamr Atieh, who took the AFM images shown here.

I would like to thank everyone who advised me over the years and helped me to accomplish this work in many ways: Dr. Jean Baum and Dr. Sagar Khare for advising this research and for mentoring me over the past few years, Dr. Wilma Olson for being on my thesis committee, Dr. Seho Kim for helpful advice when using the NMR, Dr. Valentin Starovoytov for assistance with taking TEM images, current Khare lab member Elliott Dolan for helping to get the computational symmetry protocol to work, all current members of the Baum and Khare labs, and all of my family and friends who have supported me over the years.

Table of Contents

List of Figures

List of Tables

Chapter 1: Introduction

Alpha-synuclein (asyn) is a 140 amino acid intrinsically disordered protein (IDP) that exists primarily as a monomer in vivo (Fauvet, et al. 2012) and forms inclusions that define both Parkinson's Disease (PD) and Dementia with Lewy Bodies (DLB) (Volpicelli-Daley, et al. 2011). Aggregates of asyn can also have an influence on other IDP's that cause dementia in addition to PD (Irwin, Lee, and Trojanowski 2013). The sequence of asyn is divided into three domains: a slightly positively charged N-terminal domain (residues 1-60) that forms helices in the presence of membranes, a primarily hydrophobic region known as the non-amyloid-β component (NAC) that has been strongly implicated in the mechanism for aggregation of asyn (residues 61-95), and a more negatively charged and flexible C-terminal domain (residues 96-140) (Rivers, et al. 2008; Fusco et al 2014). Current methods to design drugs to treat PD and other diseases have focused on targeting the pathway towards fibril formation as a whole (Braga, et al. 2011), but some recent drug candidates have been proposed that exploit more specific regions of the domains of asyn (Cheruvara, et al. 2015). A remaining issue which this research seeks to address is how to take a given region of asyn and, based on its known properties and interactions, propose ways to inhibit the aggregation of the full chain.

There are two other proteins homologous to asyn, but each of them have different interactions within an organism: beta-synuclein (bsyn) and gamma-synuclein (Lavedan 1998). Bsyn does not form fibrils and is also known to inhibit the formation of asyn fibrils under physiological conditions (Hashimoto, et al. 2001). When bsyn expression levels are reduced in vivo, there is a noticeable increase in asyn aggregation, suggesting that misregulation of the expression levels of asyn and bsyn leads to disease (Beyer, et al. 2011),

despite the fact that they share about 62% sequence identity (Rivers, et al. 2008). One key difference is an 11 residue stretch that is found in the NAC region of asyn and is not in the sequence of bsyn. This stretch of residues has been shown to be capable of forming fibrils outside of the context of full length asyn (Giasson, et al. 2001), although simply inserting that stretch of residues into bsyn does not seem to increase bsyn's ability to aggregate significantly (Allison, et al. 2014). These details indicate that the relatively small differences in bsyn's sequence are crucial in preventing the interactions of the full protein from being the same as asyn.

Bsyn does not completely lack the ability to form fibrils, however. Under certain conditions bsyn will be coerced into forming fibrils, including when it is in the presence of low concentrations of SDS (Rivers et al. 2008). Certain metals, such as Zn(2+), Pb(2+), and Cu(2+), will cause bsyn to form fibrils rapidly (Yamin, et al. 2005). The research performed here will additionally show that bsyn is able to form fibrils at pH 5.8 in the presence of 100 mM NaCl. This indicates that the sequence of bsyn should not be thought of as unable to form fibrils; rather, the sequence must be thought of as being far less aggregation prone and must overcome the effects of some inhibitory regions due to the influence of non-physiological conditions.

The influence of environmental conditions, particularly pH, must be considered in light of the properties of an IDP sequence like asyn's. Asyn's aggregation rate has been shown to increase at lower pH in conjunction with a decreased radius of gyration due to compaction, especially in the normally negatively charged C-terminal region (Wu, et al. 2009). The response to pH is a more general property of IDP's, since there tend to be many more charged residues than those of a completely ordered protein, and this has led to the

term “turned out” being used to describe the response of IDP’s, meaning that IDP’s actually tend to become more ordered under conditions that would normally cause a folded protein to unfold (Uversky 2009). The way to think of IDP’s under non-physiological pH in particular is that there tends to be more hydrophobicity due to charge neutralization, which leads to increased compaction that in the case of asyn and bsyn leads to faster aggregation rates.

An important aspect of the formation of amyloid fibrils that has been well established is that there must be a transition from a primarily monomeric, mostly random coil ensemble of states to a primarily beta-sheet structure (Serpell 2000). Nuclear magnetic resonance (NMR) experiments have been heavily used to probe the conformational behavior of ensembles of monomeric intrinsically disordered proteins (Jensen, Ruigrok, and Blackledge 2013), and solid state NMR (ssNMR) has been particularly useful in mapping specific regions of beta-sheet conformation along the primary sequence of fibrils of asyn (Vilar, et al. 2008). The recent combination of ssNMR and validation by electron microscopy and X-ray fiber diffraction has allowed for a full three-dimensional structure of an asyn fibril to be proposed (Tuttle, et al. 2016). The stretch of asyn spanning residues ~44 to 97 was shown to take on a particular shape known as the Greek key motif, and its image indicated how the NAC region and some specific intra- and intermolecular interactions may work to stabilize the fibrillar state. For our studies, this new fibril structure is particularly useful because its residue specific nature can allow us to propose how bsyn’s sequence is especially resistant to being in such a beta-sheet heavy conformation at specific regions.

Truncation of the C-terminal region of asyn has been shown to enhance significantly the aggregation rate of the remaining N/NAC residues (Qin, et al. 2007). Removing the N-terminal region does not seem to be as significant (Rekas, et al. 2012), although an inhibitory role has been suggested by repeated regions of the N-terminus containing the amino acid sequence KTKEGV that favor an amphipathic alpha-helix rather than beta-sheet structure (Kessler, Rochet, and Lansbury 2003). This suggests that the highly negatively charged C-terminal region inhibits fibrillation of asyn, which has been proposed to be the result of intramolecular contacts with the N-terminal or NAC region(s) that maintain its intrinsically disordered state (Hong, Dong-Pyo, et al. 2011).

Other variants of asyn such as the familial point mutants A30P, E46K, and A53T have been studied extensively, and while these are subtle changes to the primary sequence, they are known to lead to early onset PD. There are significant differences in the pathways to fibril formation that these take as well, considering that A30P actually forms fibrils at a slower rate than asyn (Lemkau, et al. 2012), but seems to favor oligomeric states that are toxic (Lázaro, et al. 2014) and still lead to the same fibril structure as wild-type asyn (Lemkau, et al. 2012; Tuttle, et al. 2016). Additional ssNMR data indicates that the E46K fibril must differ in appearance when compared with asyn and the other two familial mutants, which is likely due to the loss of a salt bridge in the Greek key structure (Tuttle, et al. 2016). Another familial mutant G51D that has been discovered and examined recently also shows increased in vitro aggregation along with other enhanced activity relative to wild-type asyn (Fares, et al. 2014). The fact that both truncations and more subtle changes in asyn's sequence can have a strong influence on its fibril forming properties means that the full sequence needs to be analyzed so as not to leave out a crucial residue.

Further complicating the comparison between asyn and its mutants/variants is that asyn can either form aggregates in a manner referred to as being on-pathway, which begins with monomer and ends in a fibrillar state, or off-pathway, where fewer monomer species form ring-shaped oligomers (Lorenzen and Otzen 2014). In terms of cell toxicity, oligomers were actually shown in vivo to be the more toxic species when a study was performed in which asyn variants that increased oligomer formation had higher toxicity than those that increased fibril formation (Winner, et al. 2011). Some researchers have even proposed that fibrils are actually a protective state relative to the more toxic oligomers in studies where oligomer formation was promoted (Chen, et al. 2009). One clear distinction between oligomer and fibril-type structures is that there is initially a higher population of helical secondary structure in aggregates relatively early in the aggregation process, but upon fibril formation the population shifts to being mostly beta-sheet (Apetri, et al. 2006). This study will focus primarily on the implications for the fibrillar state, however, since the insoluble fibril is generally seen as an end product of aggregation and is known to form the inclusions that actually define both PD and DLB (Volpicelli-Daley, et al. 2011). However, the idea that synuclein exists in a mixture of monomer, oligomer, and fibrillar states is still important to consider, since the inhibition of aggregation may occur at any stage.

A valuable approach in terms of determining what factors are most important in asyn fibril formation is to test what changes in asyn can make it more similar to bsyn in terms of lack of ability to aggregate. Recent studies have therefore focused on differences in very specific regions of both full protein sequences. These changes include using a rational design procedure to swap just 6 residues in the NAC from asyn with corresponding

ones from bsyn (Roodveldt, et al. 2012), as well as inserting the missing 11 NAC residues from asyn into bsyn as mentioned before (Allison, et al. 2014). However, what makes the problem of determining exactly what changes are responsible for making bsyn non-aggregation prone difficult is that swapping individual residues does not eliminate the toxicity of asyn and can even promote fibril formation, which has been shown by the asyn familial mutant H50Q (Appel-Cresswell et al 2013). The approach here will thus include larger swapped regions so as to maintain the context of portions of the full length protein.

One difference that can provide a major insight into the entire fibril formation pathway of asyn and bsyn has been noticed using two separate methods. In a molecular dynamics study, it was determined that bsyn monomer was able to bind asyn monomer with a lower energy than asyn monomer binding to itself (Tsigelny, et al. 2007) and that binding of asyn by bsyn primarily occurred in a head-to-tail manner, while asyn homodimers were able to adopt both head-to-tail and head-to-head conformations. Only the latter arrangement seemed to propagate towards aggregation. A recent study utilizing paramagnetic relaxation enhancement (PRE) in an exclusively intermolecular manner was able to show via long-range contacts that in an ensemble containing both asyn and bsyn, the head-to-tail conformation was primarily able to be detected, while in ensembles of asyn alone, both the head-to-head and head-to-tail conformations were evident (Janowska, et al, 2015). Bsyn showed much lower propensity in terms of interactions to make bsyn-bsyn dimers, and the small amount that was seen was primarily head-to-tail. The interaction profiles in each case indicate the importance of N-terminal to C-terminal intermolecular interactions in the earliest stages of fibril formation that may influence how the NAC region is able to become tightly ordered later in the pathway.

In an attempt to get a better sense of the disparity between asyn and bsyn's behaviors, our group conducted a study where 6 individual point mutants in the N-terminal region were made in the sequence of asyn for the corresponding position in bsyn so that the effect of each individual residue on the aggregation of asyn could be probed. The major conclusion that could be drawn was that certain changes may decrease the aggregation of asyn slightly, but the mutants H50Q and T54S both had noticeably faster rates of aggregation. Transmission electron microscopy (TEM) also indicated that there is not a simple relationship between lag times and fibril morphology, so looking at the fibrils did not help to explain why certain mutations increased or decreased the rate of aggregation compared to asyn. The discovery that the mutant T54S, which is a highly conserved mutation between the two sequences, could actually cause a significant increase in asyn's aggregation rate led our group to take a more general approach.

Since analyzing the effect of each individual mutation did not seem to give a thorough comparison between asyn and bsyn's N-terminal regions, as well as the fact that there are many point mutations when aligning the NAC (residues 61-95 in asyn, 61-85 in bsyn) and C-terminal (residues 96-140 in asyn, 86-134 in bsyn) regions, our group decided to start analyzing the effect that each domain has in the context of both full length proteins. This meant that each combination of domains had to be tested, where each letter stands for one of the three domains from the corresponding wild type protein: AAA, AAB, ABA, BAA, BAB, ABB, BBA, and BBB (full sequences shown in Figure 1.1). Using mutagenesis as well as a technique known as Gibson assembly (Gibson 2009), proteins containing each of these combinations of asyn and bsyn sequences, or chimeras, were expressed from a plasmid DNA containing the proper nucleotide sequence. This approach

was determined based on the idea that individual stretches of bsyn's sequence could inhibit the aggregation of asyn, including peptides from bsyn's N-terminus (Windisch, et al. 2004) and the region of bsyn from residues 36 to 46 (Shaltiel-Karyo, et al. 2010). Similar chimeras were also explored in the literature under different conditions and with slightly different sequences than described here (Zibaee, et al. 2007), which revealed that simply including residues from bsyn in the context of asyn could inhibit aggregation of the rest of the otherwise aggregation-prone sequence. The crucial differences between our approach and previous approaches are that the influence of each domain was able to be determined simultaneously and the chimera sequences included every residue for each domain, since previous studies had already shown that leaving out particular residues in the NAC region could significantly alter the aggregation behavior of the full protein (El-Agnaf and Irvine 2002).

Figure 1.1 Aligned Sequences of Chimeras with Asyn/Bsyn. Each sequence shown corresponds to one of the chimera sequences aligned with asyn or bsyn, along with the wild-type sequences on the top and bottom. Blue letters indicate N-terminal amino acids, red letters indicate NAC amino acids, and gold letters indicate C-terminal amino acids.

The methods employed here were primarily intended to determine the rates of aggregation of each chimera and compare with the control wild-type proteins, as well as to see if there were any differences in the monomeric ensembles of states and the overall appearance of the fibrillar end-products. The thioflavin T (ThioT) binding assay (Khurana, et al. 2005) was employed to study aggregation rates due to the affinity of ThioT for fibrillar structures and shows a significant increase in its fluorescence intensity upon binding. NMR methods were primarily focused on determining chemical shift differences (CSD's) for ABA and BAB specifically, which can be used to determine simply that there are differences in the monomeric ensembles of states relative to the wild-type counterparts for each domain (Jensen, Ruigrok, and Blackledge 2013). After completion of the ThioT assay, the fibrils obtained from samples that were able to show significant ThioT intensity changes were bound to a mica surface and imaged by Atomic Force Microscopy (AFM). This technique has been used specifically in the context of asyn's C-terminal region in order to determine fibril height changes as a result of solution conditions and to analyze its flexibility (Sweers, et al. 2012), so analysis of fibril morphology was done in order to detect any possible influence in the way that each domain can alter the appearance of the fibril end-product. Performing simulations where the sequence of bsyn was threaded onto the fibril structure obtained from PDB 2n0a (Tuttle, et al. 2016) including only residues 30 to 97 showed which particular residues were able to stabilize or destabilize the Greek key motif and were used to illustrate ways that a bsyn NAC could possibly compensate for its lack of crucial residues.

This study will show that chimeras with a bsyn NAC region (XBX) require a reduction in pH to form fibrils, while XAX chimeras are more similar to asyn in their

aggregation behavior and possibly energetics within the Greek key fibril conformation. The asyn N-terminal to bsyn C-terminal interactions seemed especially inhibiting, but the bsyn N-terminal to asyn C-terminal seemed to be the same or possibly even more fibril prone than wild-type asyn. There also seemed to be some border effects where, for example, the asyn NAC may have a slight allosteric effect on a short region of bsyn residues (~55-60). This information led to the conclusion that inhibiting asyn aggregation may be most effectively done with peptides specifically derived from bsyn's C-terminal region and in general the region before asyn's NAC may not be able to remain stable in the Greek key conformation when allosteric effects are induced. Both of these regions thus serve as a type of threshold for fibril formation that must be overcome in the case of bsyn through the presence of non-physiological conditions that induce conformational changes.

Chapter 2: Materials and Methods

Chapter 2.1 Introduction

The protocols that will be described here include techniques such as mutagenesis and Gibson cloning, with protein expression and purification performed as described previously, as well as the protocol for taking TEM images of the N-terminal point mutants (Kang, et al. 2011). ThioT aggregation assays, AFM, and NMR HSQC methods used to collect all experimental data will then be described in detail. The protocol needed to perform simulations of wild-type and chimera fibril structures will also be described in detail.

Chapter 2.2 Chimera Preparation Protocol:

Materials:

1. Gibson Master Mix (New England BioLabs, Ipswich, MA).
2. Q5 Reaction Buffer (New England BioLabs, Ipswich, MA).
3. 10 mM DNTPs (Life Technologies, Carlsbad, CA).
4. Pfu Ultra High-Fidelity DNA Polymerase (Agilent Technologies, Santa Clara, CA).
5. G-block fragments (for AAB, BAB, BBA, and ABA) (Integrated DNA Technologies, Coralville, Iowa).
6. Primers (for BAA and ABB only) (Integrated DNA Technologies, Coralville, IA).
7. GeneJET Plasmid Miniprep Kit (Thermo Fisher Scientific, Waltham, MA).
8. Luria Broth (Sigma Aldrich, St. Louis, MO).
9. QIAprep Spin Miniprep Kit (Qiagen, Valencia, CA).

Primers Needed to Obtain Linearized Vectors

AAB:

Forward: TAAGAAATATCTTTGCTCCCAGTTTCTTGAGATCTGC

Reverse: GACAAAGCCAGTGGCTGCTGCAATGC

BBA:

Forward: TAGAAGCTTGCGGCCGCACTCGAGC

Reverse: CTTCACCAGTCCTGTGGCTGCTGCG

BAB:

Forward: AGGGAGGAATTCCCTACTGATCTGA

Reverse: CTTGGTTTTTTCAGCCACTGAAGCC

ABA:

Forward: AAAAAGGACCAGTTGGGCAAGAATG

Reverse: TTTGGTCTTCTCAGCCACTGTTGCC

G-Block fragments used:

AAB:

GGGAGCATTGCAGCAGCCACTGGCTTTGTCAGGGAGGAATTCCCTACTGATC
TGAAGCCAGAGGAAGTGGCCCAGGAAGCTGCTGAAGAACCACTGATTGAGC
CCCTGATGGAGCCAGAAGGGGAGAGTTATGAGGACCCACCCCAGGAGGAAT
ATCAGGAGTATGAGCCAGAGGCGTAAGAAATATCTTTGCTCCCAGTTTCTTG
A

BBA:

AACATCGCAGCAGCCACAGGACTGGTGAAGAAAAAGGACCAGTTGGGCAAG
AATGAAGAAGGAGCCCCACAGGAAGGAATTCTGGAAGATATGCCTGTGGAT

CCTGACAATGAGGCTTATGAAATGCCTTCTGAGGAAGGGTATCAAGACTACG

AACCTGAAGCCTAGAAGCTTGCGGCCGCACTCGAGCACCAC

BAB:

GGTGTGGCTTCAGTGGCTGAAAAAACCAAGGAGCAAGTGACAAATGTTGGA

GGAGCAGTGGTGACGGGTGTGACAGCAGTAGCCCAGAAGACAGTGGAGGGA

GCAGGGAGCATTGCAGCAGCCACTGGCTTTGTCAGGGAGGAATTCCCTACTG

ATCTGAAGCCA

ABA:

GGTGTGGCAACAGTGGCTGAGAAGACCAAAGAACAGGCCTCACATCTGGGA

GGAGCTGTGTTCTCTGGGGCAGGGAACATCGCAGCAGCCACAGGACTGGTGA

AGAAAAAGGACCAGTTGGGCAAGAATGAAGAA

Primers for BAA and ABB:

BAA Forward (For K10M mutant of Asyn):

ACCAAACAGGGTGTGACAGAAGCAGCAGAAAAGACAAAAGAGGGTGTTCTC

TATGTAGGCTCCAAAACCAGGGAGGGAGTGGTGCAAGGTGTGGCATCAGTGG

CTGAGAAGACC

BAA Reverse (For K10M mutant of Asyn):

GGTCTTCTCAGCCACTGATGCCACACCTTGCACCACTCCCTCCCTGGTTTTGG

AGCCTACATAGAGAACACCCTCTTTTGTCTTTTCTGCTGCTTCTGTCACACCCT

GTTTGGT

ABB Forward (For M10K mutant of Bsyn):

ACCAAGCAGGGGGTCGCCGAGGCGGCGGGGAAGACCAAGGAGGGCGTCCTC

TACGTCGGAAGCAAGACCAAAGAAGGTGTGGTACACGGTGTGGCTACAGTG

GCTGAAAAAACC

ABB Reverse (For M10K mutant of Bsyn):

GGTTTTTTCAGCCACTGTAGCCACACCGTGTACCACACCTTCTTTGGTCTTGCT

TCCGACGTAGAGGACGCCCTCCTTGGTCTTCCCCGCCGCCTCGGCGACCCCCT

GCTTGGT

Methods:

First, the wild type vectors need to have the appropriate nucleotides removed by PCR to form a new, linear vector that does not contain that particular domain.

Table 2.1. Amounts to Add to Each Tube to Obtain Linearized Vector (can multiply by 4 and portion ~50uL each into PCR tubes):

5X Q5 Buffer	10 uL
10 uM DNTP's	1 uL
10 uM Forward Primer	2.5 uL
10 uM Reverse Primer	2.5 uL
Template	1 uL
DNA Polymerase	0.5 uL
Water	37.8 uL

After verifying that the vector has been linearized by agarose gel electrophoresis, use GeneJET PCR purification kit to purify the linear vector.

PCR to Obtain Linear Vectors:

Preheat lid: 105 ºC

Initial Denature: 98.0 ºC 30 sec.

Cycle (25x):

1. 98.0 ºC; 10 sec.
2. ~3 ºC below Tm determined by IDT DNA OligoAnalyzer Tool with 2 mM MgSO4; 30 sec.
3. 72.0 ºC; 1 min.

Final extension: 72.0 ºC; 2 min, then Hold 4 ºC

Table 2.2. Gibson Reaction Setup:

Linearized Vector	1.5 uL (Diluted 10X)
G-Block Insert	3.0 uL (20ng/uL)
Water	5.5 uL
Master Mix	10 uL

Add components to a PCR tube and incubate at 50ºC for 15 minutes. Transform 7 or 8uL of the reaction mixture into DH5α cells. After taking a colony from the plate and growing overnight in 5 mL LB with proper antibiotic, use a QIAprep Spin Miniprep Kit to purify resulting plasmid.

Note that mutagenesis was also performed in a similar manner to obtain the mutants K10M, A27T, G31E, K45R, H50Q, and T54S with the appropriate primers.

Chapter 2.3 Thioflavin T Binding Protocol:

Materials:

1. Thioflavin T (ThioT) (Acros Organics, Pittsburgh, PA).
2. 0.22 um filter (Millipore, Billerica, MA).
3. PTFE beads (Saint-Gobain, Malvern, PA).
4. Compressed air (Falcon Safety Products, Branchburg, NJ)
5. POLARstar Omega Fluorimeter (BMG Labtech, Cary, NC).
6. MES/MOPS pH 5.8 or pH 7.3 buffer (Components from Sigma Aldrich Aldrich, St. Louis, MO).

Methods:

1. Prepare 2 mM Thioflavin T and filter through a 0.22 um filter.
2. Pass compressed air over each well of a 96 well microplate to remove any particles inside.
3. Place a Teflon bead in each well that will have protein sample.
4. Take 97 uL of 70 uM protein in either MES/MOPS pH 5.8 or pH 7.3 buffer and pipette into the appropriate wells.
5. Let shake at 37ºC and 600 rpm (Protein Aggregation method) until all fluorescence curves appear to have plateaued (~300 hours in this case).
6. Immediately store plate at 4ºC when run is complete.
7. Note that for the N-terminal point mutants, used a concentration of 50 uM, temperature of 23ºC, and used a PBS pH 7.4 buffer (components from Sigma-Aldrich, St. Louis, MO).

Chapter 2.4 Atomic Force Microscopy (Protocol performed by Tamr Atieh):

Materials:

1. Protein fibril from ThioT experiment.
2. NX-10 instrument (Park systems, Suwon, South Korea).
3. PPP-NCHR non-contact mode tips (Nanosensors, Neuchatel, Switzerland).
4. Mica sheets (Ted Pella Inc, Redding, CA).

Methods:

1. Determine remaining volume of solution in the well after completing the ThioT experiment and add buffer to adjust back to 97 uL.
2. Pipette into a 1.5 mL tube and vortex to ensure that fibril is suspended in solution.
3. Pipette 20 uL of the solution onto a 1cmx1cm square of freshly cleaved mica.
4. Allow to incubate for 5-10 minutes while the mica is covered.
5. Wash the surface of the mica 3 times with 100 uL of water and dry bottom and edges with filter paper.
6. Allow surface to air-dry for 1 hour before imaging on an NX-10 microscope with non-contact mode tips (PPP-NCHR, force constant 42 N/m; 330 kHz frequency).
7. Process images using Gwyddion software.

Chapter 2.5 Generating Computational Fibril Models (Assistance provided by Elliott Dolan):

Protocol:

1. Loaded structure 2n0a.pdb into PyMol, which was the published structure of the asyn fibril in a Greek key conformation (Tuttle, et al. 2016).

2. Removed chains A, B, H, I, and J so that only 5 chains from the middle would be present.

3. Removed residues 1-29 and 98-140 from all chains to eliminate disordered regions.

4. Made a symmetry definition file with the script make_symmdef_file.pl (Dimaio, et al. 2011) to create a symmetric input pdb file for use in Rosetta 3.6 (Leaver-Fay, et al. 2011).

5. Created a RosettaScripts input xml file to mutate the desired residues to match the sequence of bsyn or to keep the sequence the same as asyn's.

6. Specified atom coordinate constraints in the xml so that all backbone atoms in each chain would have a maximum rms of 0.2 angstroms from the solid-state NMR structure.

7. Used Rosetta's Symmetric Fastrelax algorithm on the structure with mutated sequence to generate 1000 output pdbs.

8. Removed the 0.2 angstrom rms limit to allow the structure to be refined without constraints.

9. Used Rosetta's Symmetric Fastrelax algorithm to produce 4000 refined structures without constraints.

Chapter 2.6 NMR Chemical Shift Differences Protocol:

Materials:

1. N15 labeled protein
2. MES/MOPS with 100mM NaCl pH 5.8/7.3 (Components from Sigma Aldrich).
3. D2O (Sigma Aldrich, St. Louis, MO).
4. Amicon 100 kDa/3kDa filters (Millipore, Billerica, MA).

5. NMR Spectrometer (Bruker, Billerica, MA).

Protocol:

1. Dissolve N15 labeled protein in MES/MOPS pH 7.3.
2. Pass through an Amicon 100 kDa filter (Millipore, Billerica, MA) to remove higher order aggregates.
3. Buffer exchange 5x into MES/MOPS pH 5.8 100 mM NaCl after transferring to a 3 kDa filter or simply wash 4x with MES/MOPS pH 7.3.
4. Concentrate to 300 uM concentration in ~350 uL buffer in a Shigemi tube (Allison Park, PA).
5. Perform HSQC on 600 MHz Bruker spectrometer at both pH 5.8 and 7.3 (for ABA and BAB proteins only).
6. Determined chemical shift differences with a scaling factor of (0.35)^2 for N15 shifts.

Chapter 3: Chimera Experiments Reveal that Bsyn's C-terminal Domain and a Region Near the Start of the NAC Provide a Threshold for Fibril Formation that Depends on the pH of its Environment

Chapter 3.1 Point Mutations in N-terminal Region of Asyn Indicated Importance of Examining Asyn to Bsyn Changes with Sequence Context

Initially, our group came up with a hypothesis that any mutation from asyn to bsyn in the N-terminal region should likely be inhibiting with the exception of H50Q, since that mutation seems especially non-conserved. However, as seen in the plot below (Figure 3.1), the T54S mutation seems to be significantly close to the H50Q mutation in terms of lag time, despite being a much more conserved mutation. TEM images (Figure 3.2) of the fibrils simply indicated that fibril morphology did not seem to be easily predictable based on the aggregation rates or the position of the mutation in asyn's sequence, considering that K45R and T54S appear to have similar looking fibrils and yet have very different lag times. These observations made clear that there must be certain parts of bsyn's sequence that offset the fairly aggregation prone regions by providing some inhibition, which led us to the chimera approach that makes sure to include at least the context of each of the domains.

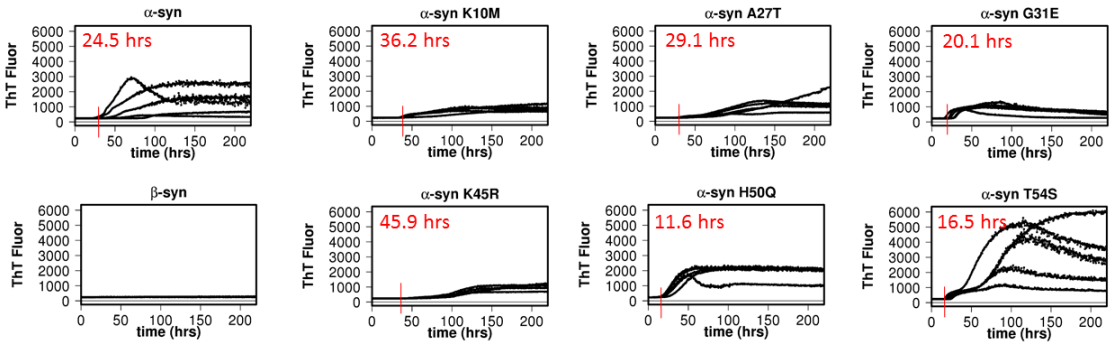

Figure 3.1. Thioflavin T Curves With Estimated Lag Times for N-terminal Mutants of Asyn. Shown in each plot is the raw fluorescence intensity for asyn, bsyn, and the 6 N-terminal mutants of asyn versus the number of hours of incubation. Indicated in the upper left hand corner of each plot (except bsyn) is the estimated lag time for each sample with a bar to indicate roughly when the intensity begins to increase significantly.

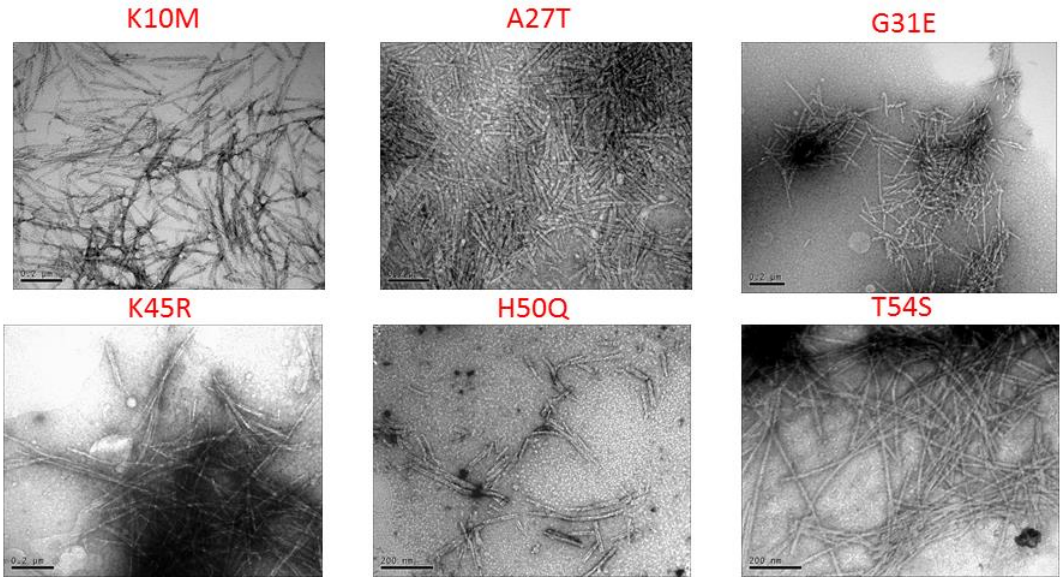

Figure 3.2 TEM Images of N-terminal Point Mutants. Representative TEM images of each of the N-terminal point mutants for one of the samples from the Thioflavin T assay shown in Figure 3.1. Scale bars are indicated in the bottom left corner and are 0.2 um (or 200 nm).

Chapter 3.2. Chimera Fibril Formation Assay Shows that the NAC is the Region that Determines Aggregation Behavior When Considering Environmental Conditions and Modulation by the Flanking Domains

To determine the influence that each domain has on the ability of asyn/bsyn to form fibrils, ThioT binding assays served as a way to monitor when fibrils actually started to form in each case. The ThioT binding assay makes apparent that the XAX chimeras are able to form fibrils at pH 5.8 and 7.3, while the XBX chimeras appear to form fibrils only at pH 5.8 (Figure 3.3). This confirms that the bsyn NAC region can act as a pH sensitive switch in terms of its aggregation behavior. The XAX chimeras are able to form fibrils more rapidly at pH 5.8 as well, with noticeably less differences in lag times when compared to the XBX chimeras.

The flanking regions appear to have regulatory roles for the chimeras. Interestingly, the bsyn N-terminal region does not seem to have an inhibitory effect and may even accelerate fibril formation, as is shown by how similar the lag time for BAA is compared to asyn. The C-terminal region of bsyn seems to have a greater inhibitory effect than asyn's C-terminal region, especially in the case of ABB and AAB, where asyn's N-terminal region is interacting with bsyn's C-terminal region.

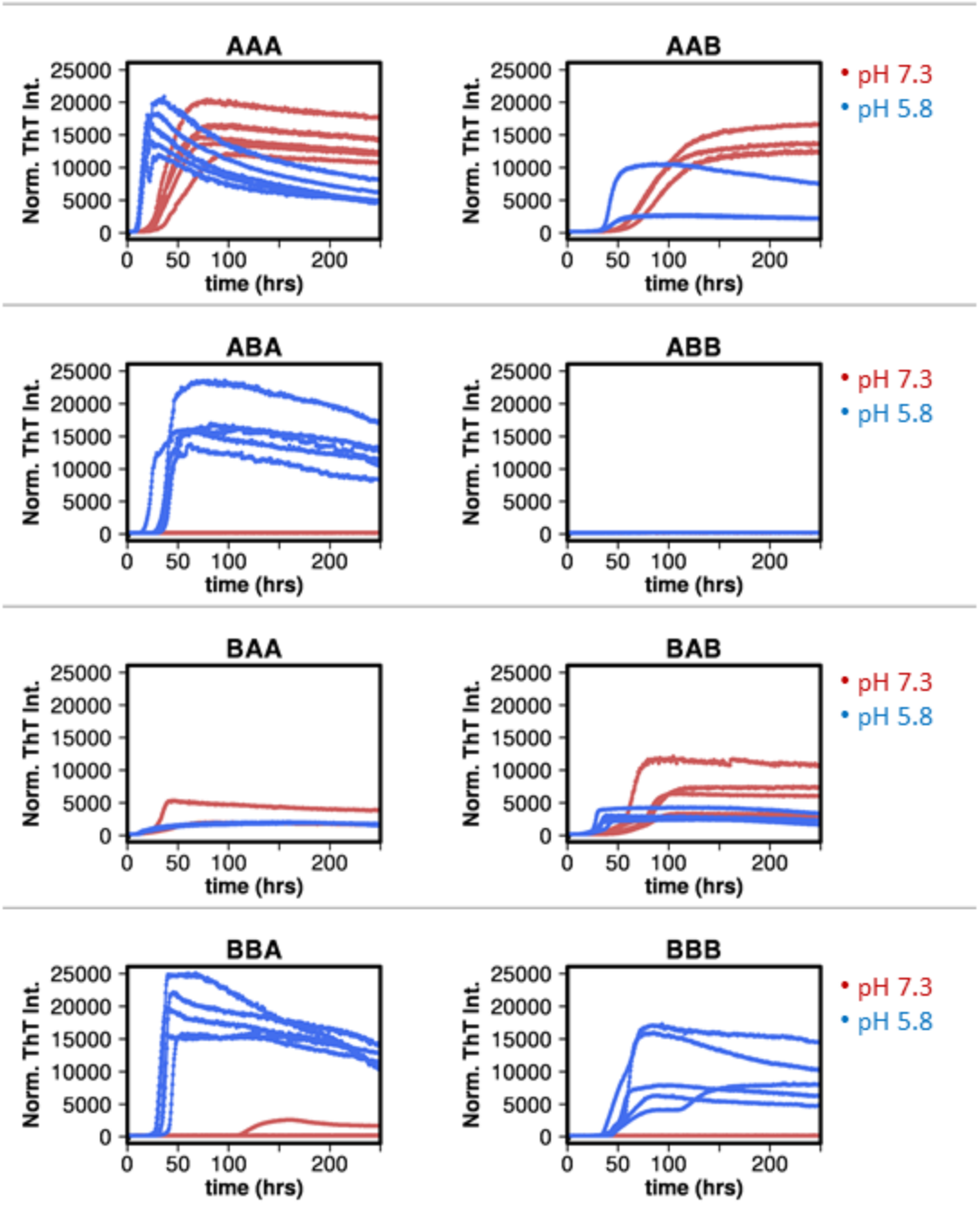

Figure 3.3. ThioT Fibrillation Kinetics of asyn/bsyn and chimeras at pH 7.3 and 5.8. Shown in each plot are raw fluorescence intensity versus number of hours of incubation for different wells containing asyn, bsyn, and each of the chimeras. Red curves

correspond to samples at pH 7.3, while blue curves correspond to samples at pH 5.8. Figure prepared by Gina Moriarty.

An important distinction between the XAX and XBX samples is that while a pH decrease always increases aggregation rates, the bsyn NAC is clearly acting like an on/off switch. In both cases, the increased hydrophobic packing can be considered to increase aggregation rates, since the proteins themselves are becoming more compact rather than extended, but the bsyn NAC molecules seem to be able to access at least one type of conformation exclusively at lower pH that allows them to exist in some other fibrillar structure, most likely not in the Greek key. The inhibition from the flanking regions, then, is most likely due to intermolecular interactions that define earlier portions of the aggregation pathway, especially dimer formation. The asyn N-terminal to bsyn C-terminal interaction seems to be the most inhibiting, especially considering the case of ABB, which did not form fibrils at either pH in this case. This distinction between how the NAC and the flanking regions affect the aggregation pathway is critical, since it can explain why a sample like AAB actually tends to form fibrils more slowly than BAB, even though AAB appears by computation (as will be shown in Figure 3.8) to be slightly more stable in the Greek key fibril state. It is also critical to note that in the case of ABB, it is likely that increasing the concentration would allow it to form fibrils, but higher concentrations were not tested here.

Chapter 3.3 AFM Imaging of the Chimera and Wild-type Proteins Reveals Morphological Differences that Further Demonstrate the Influence of Regions Flanking the NAC and the Influence of pH Changes

Qualitative differences in fibril morphologies can provide insight into how the fibrils tend to come together, so the fibrils were imaged by AFM (performed by Tamr Atieh) in this case for one well for each of the samples that had a significant increase in fluorescence intensity. The representative AFM images of the chimera and wild-type proteins (Figure 3.4) consistently appear shorter at pH 5.8, indicating that the environmental conditions are a crucial factor in determining the extended fibril structure regardless of sequence. The flanking domains appear to have an additional effect that is not obvious when comparing lag times, which is to guide the shape of the full fibril. The ABA samples form thin, extended strands, while BBA's are thicker and not as long, like asyn's at pH 7.3. BAB and BAA both appear to resemble asyn at pH 5.8 and 7.3, although BAA's may tend to be slightly shorter at pH 7.3. This supports the idea mentioned before that bsyn's N-terminus is not inhibiting and instead may promote fibril formation.

The inhibition induced by bsyn's C-terminus appears to be evidenced here as well. AAB's fibrils seem to be bundled more than asyn's at pH 7.3, and at pH 5.8 the fibrils appear to be overlapping and bundled even more extensively. ABB did not have visible fibril at either pH and instead seems to have taken on smaller, probably oligomeric, aggregates.

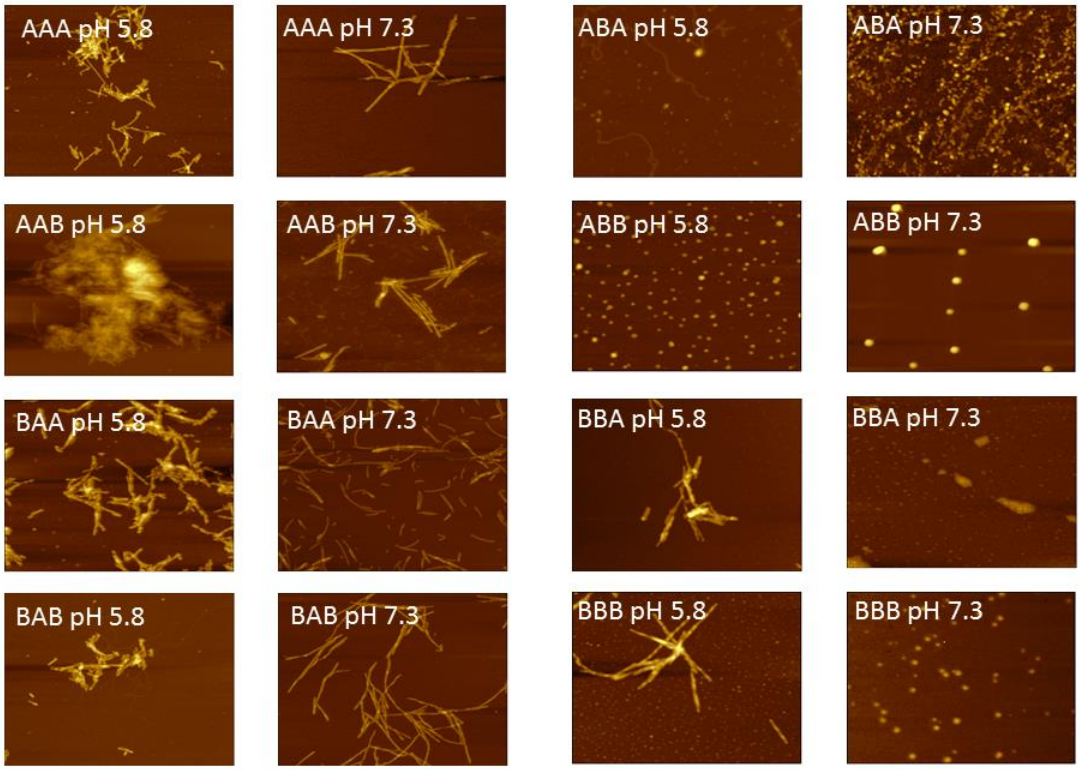

Figure 3.4. AFM images for asyn, bsyn, and all chimeras at pH 5.8 and 7.3. Shown in A) through P) are representative AFM images (2.5nm x 2.5nm) with the corresponding pH indicated. Darker colors correspond to smaller relative heights, while brighter colors correspond to larger relative heights. Images were obtained by Tamr Atieh.

The AFM images are valuable in capturing differences in representative images of each of the actual fibrils the chimeras form, particularly supporting the notion from Chapter 3.2 that the bsyn N-terminal region actually enhances fibril formation, while the bsyn C-terminal region is more likely to prevent advancement beyond oligomeric states. Note that this does not mean the bsyn C-terminal region prevents cell toxicity, since the oligomers themselves are possibly more toxic to cells, even the ones that are considered

off-pathway as discussed in Chapter 1. However, it is clear that enhancing antiparallel interactions between asyn's N-terminal region and a ligand similar to bsyn's C-terminal region could at least help to prevent the advancement to fibril, and the increase in oligomers would be a side effect.

Chapter 3.4 Chemical Shift Differences Between the ABA and BAB Monomeric Ensembles Indicate a Possible Allosteric Influence of the NAC region on Residues ~55 to 60

Since chemical shifts are dependent on the chemical environment in which an amino acid is located, looking at Chemical Shift Differences (CSD's) can provide valuable insights into changes in the conformational space that a protein samples on average compared to a wild-type distribution. In this case, our group wanted to check at least the effect of exchanging NAC regions on the monomeric ensemble, and thus only ABA and BAB were studied. CSD plots (Figure 3.5) taken from 1H-15N HSQC spectra of the chimeras ABA and BAB appear to have only small changes at certain residues where the sequence is the same as the corresponding wild-type protein. The monomeric ensembles in a qualitative sense, then, can be thought of as sampling space in a similar way for the residues from the corresponding wild-type protein and there are likely not any large unexpected changes in overall structure that result from the juxtaposition of domains. At residues ~55 to 60 in ABA at pH 5.8 and BAB at both pH's, however, there is an increasing trend in the CSD's as well as a visible change in the positions of those peaks in the 1H-15N HSQC spectra (Figure 3.6). Since this trend is only noticeable when comparing ABA with asyn at pH 5.8 and is seen at both pH's when comparing to BAB to

bsyn, although with a lower magnitude at pH 7.3, there may be a conformational shift for the monomeric ensemble that occurs in conjunction with the ability to form fibrils for these arrangements of the domains. ABA at pH 7.3 does have some visible changes near residue 60, but they are less significant than the rest and do not result in a persistent increase in CSD's. Note that any other differences that can be seen in the CSD plots are either the result of point mutations or are most likely the result of peaks being less overlapped in the chimera compared to the wild-type spectrum.

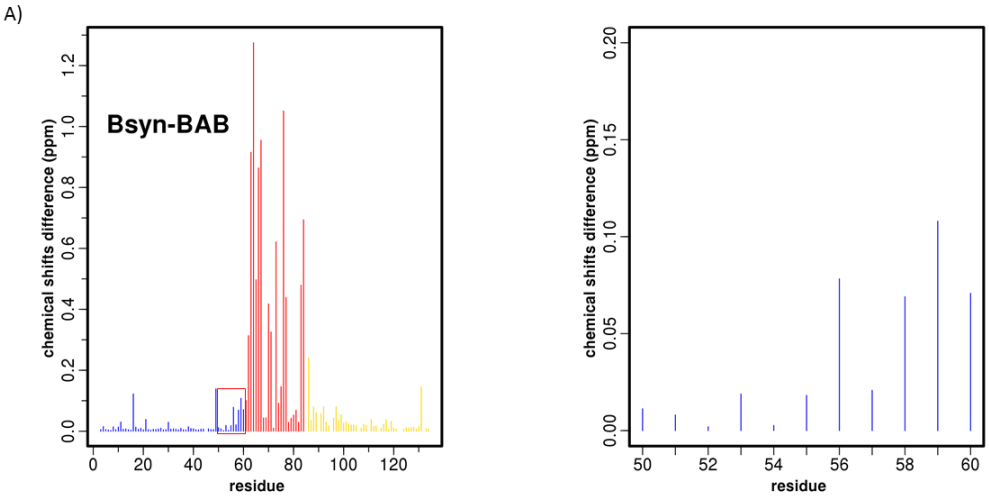

pH 5.8

B)

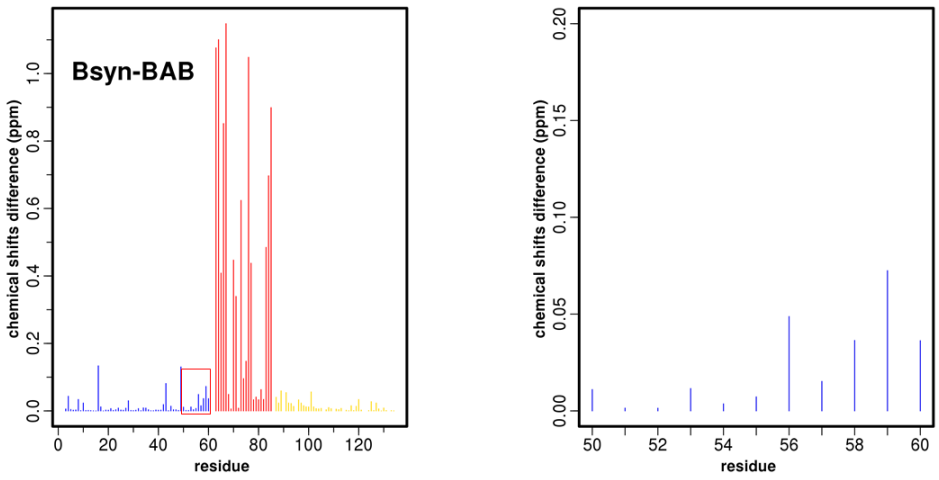
Bsyn-BAB
chemical shifts difference (ppm)
residue
0.0
0.2
0.4
0.6
0.8
1.0
0
20
40
60
80
100
120
0.00
0.05
0.10
0.15
0.20
50
52
54
56
58
60

pH 7.3

C)

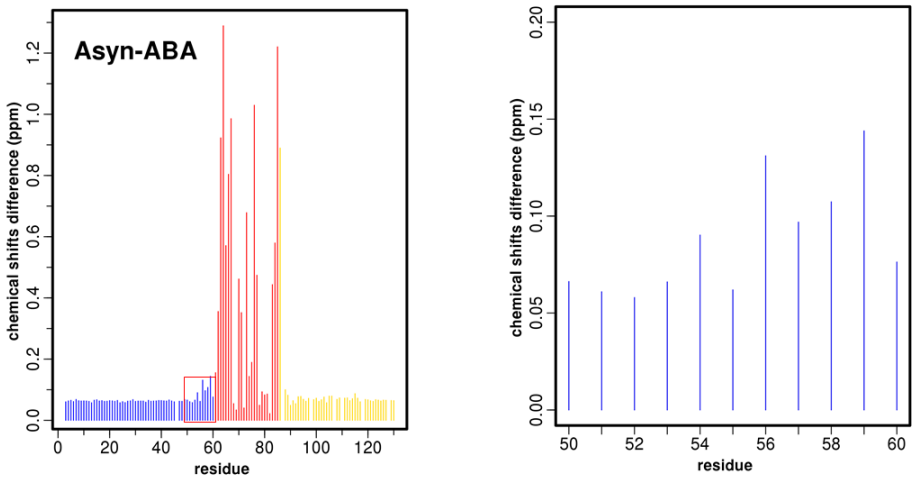
Asyn-ABA
chemical shifts difference (ppm)
residue
0.0
0.2
0.4
0.6
0.8
1.0
1.2
0
20
40
60
80
100
120
0.00
0.05
0.10
0.15
0.20
50
52
54
56
58
60

pH 5.8

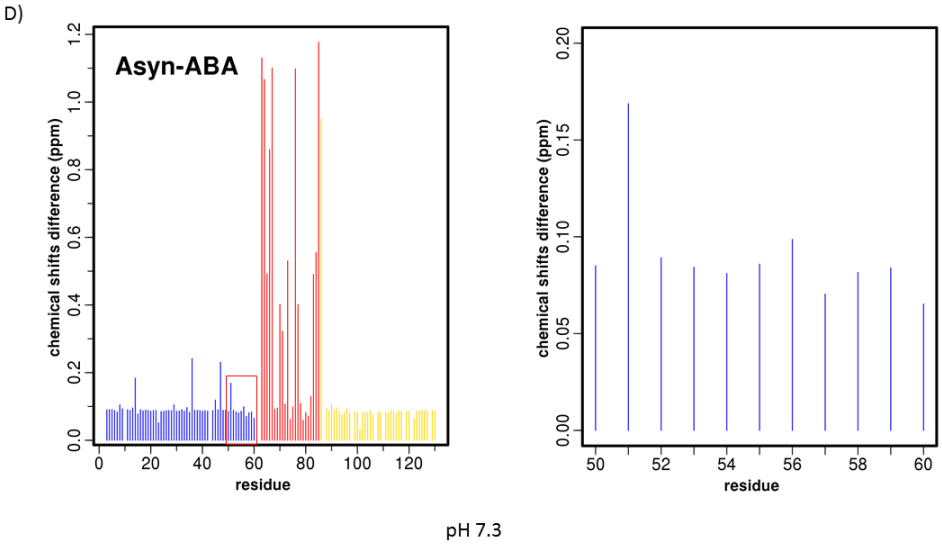

Figure 3.5. ABA and BAB HSQC CSD Plots. A) and B) show plots of CSD versus residue number for bsyn compared to BAB at pH 5.8 and 7.3, respectively. C) and D) are plots of CSD versus residue number for asyn compared to ABA at pH 5.8 and pH 7.3, respectively. The panel on the right magnifies the region indicated in the red rectangle for clarity. The blue bars indicate CSD's for N-terminal residues, red bars indicate NAC residues, and gold bars indicate C-terminal residues.

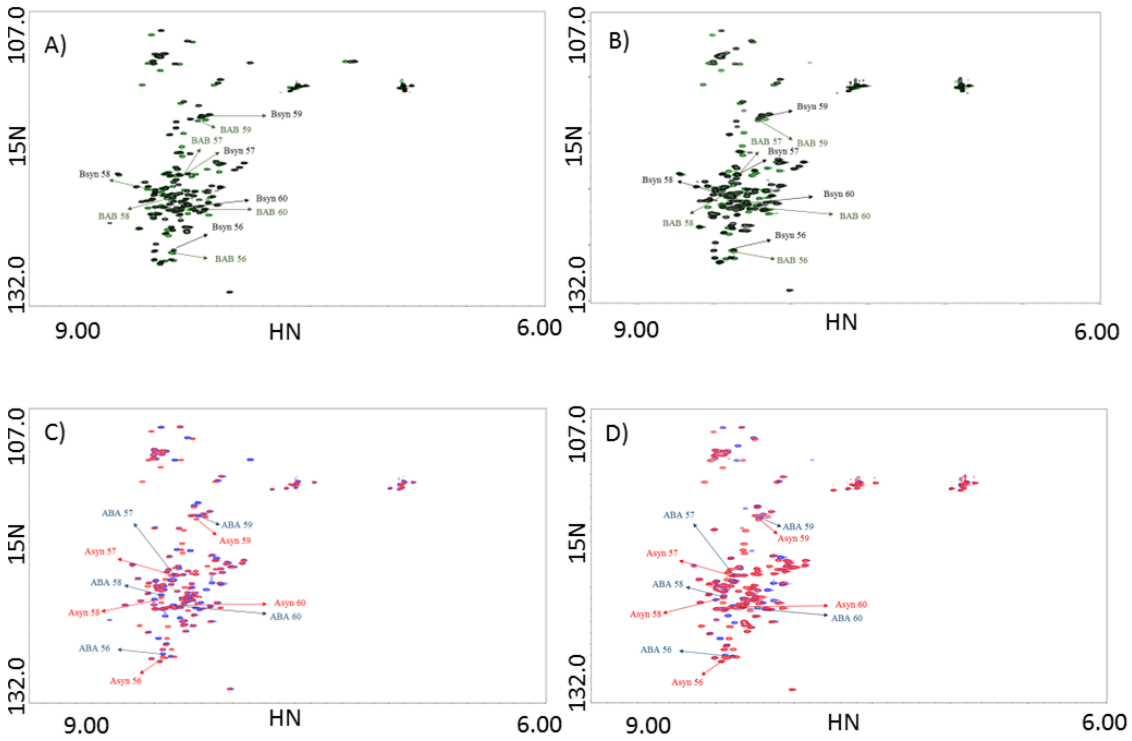

Figure 3.6. ABA and BAB HSQC comparisons with asyn/bsyn. The HSQC spectra in A) and B) correspond to bsyn overlaid onto BAB at pH 5.8 and 7.3, respectively. Asyn peaks are overlaid onto ABA at pH 5.8 and pH 7.3 in C) and D), respectively. The arrows indicate where residues 56-60 are located. The y-axis corresponds to 15N chemical shifts (from ~107.0 to 132.0 ppm) and the x-axis to 1H chemical shifts (from ~6.00 to 10.00 ppm).

The score per residue plots (Figure 3.7) for the chimeras compared to the wild-type structures with constraints appear to have a trend that makes them more similar to the neighboring wild-type domain at residues ~55 to 60 as well. The changes in fibril score near residue 46 are particularly hard to compare with the NMR spectra due to

considerable overlap of their peaks, and any changes from residue 30 to 33 can be attributed to the fact that they are near the completely disordered part of the protein and thus are not as rigidly held in place as the Greek key part of the fibril.

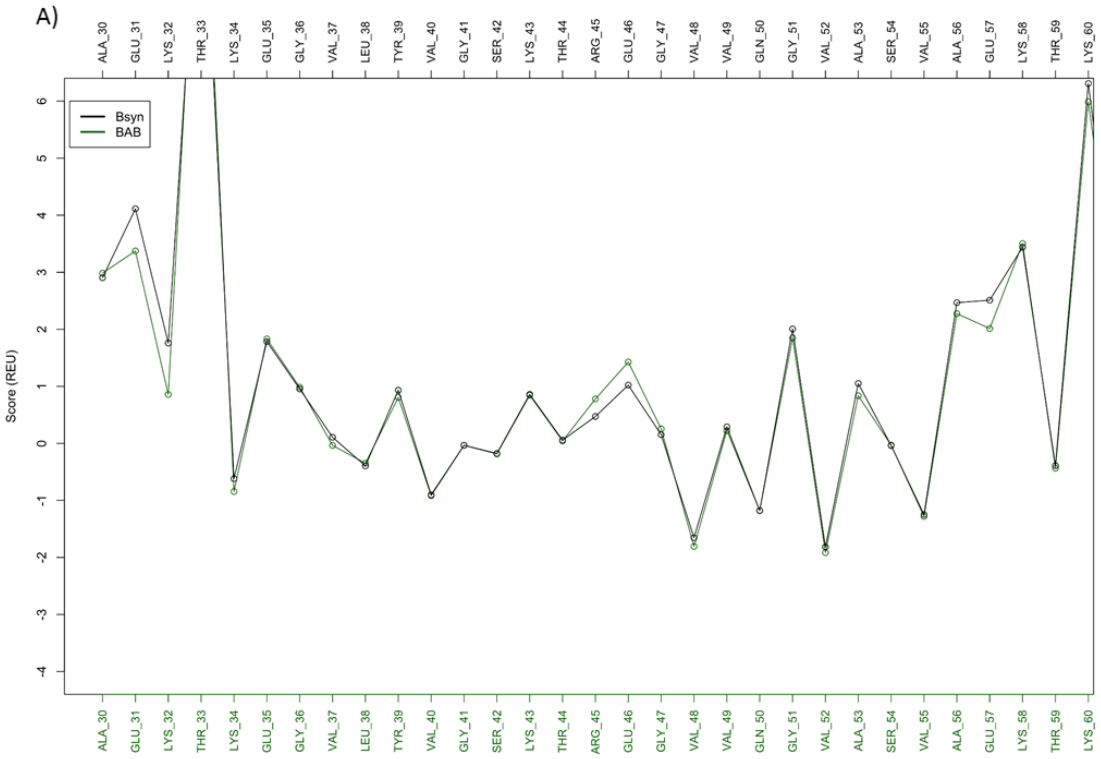

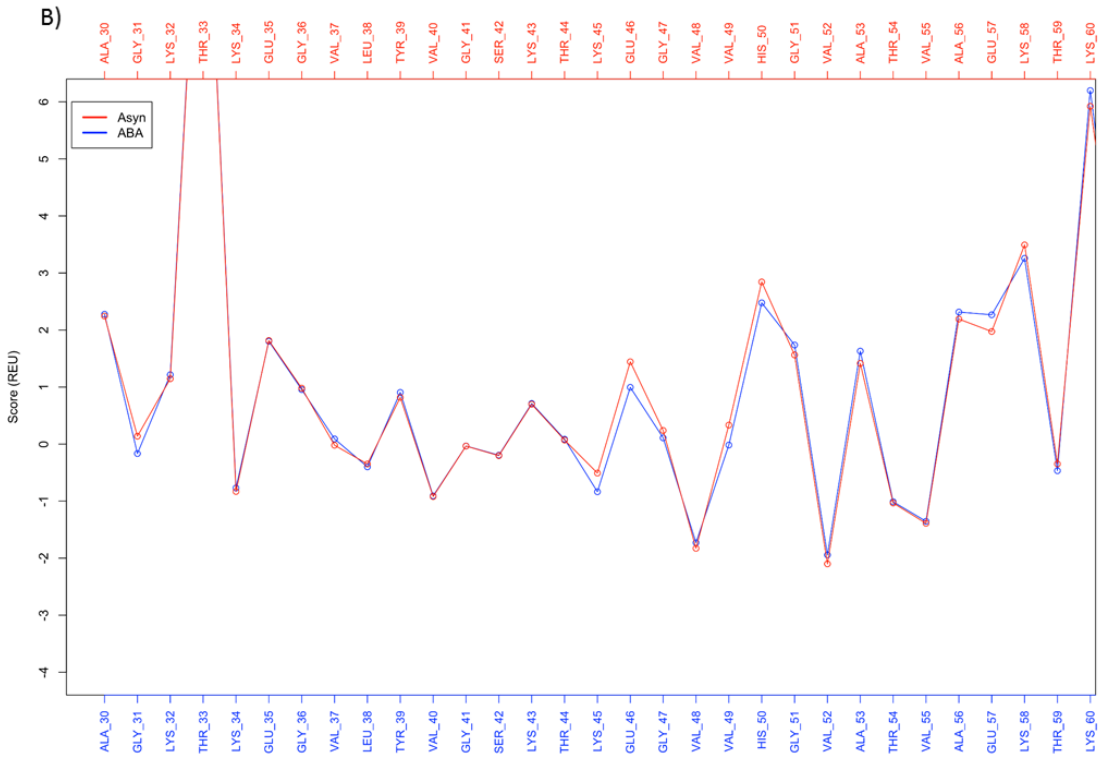

Figure 3.7. Score per residue plots for bsyn/BAB and asyn/ABA. The green and black curves shown in A) correspond to the average score in Rosetta Energy Units (REU) over 1000 pdb files versus a residue from positions 30-60 for BAB and bsyn, respectively. The red and blue curves in B) correspond to Asyn and ABA, respectively.

The NMR results seem to indicate at least some influence of the juxtaposition of domains, which is seen more clearly when looking at the energies per residue for the constrained chimera structures. The scores near residues ~55 to 60 appear to be close to or exactly the same as the corresponding position for the protein in the neighboring region. Thus, it is possible that there are some subtle allosteric effects, although NMR may not be sensitive enough to detect all of them. These per residue energies are purely

for the fibril state as well, so it could be that any allosteric differences specific to the chimeras do not become noticeable until closer to the actual formation of the fibril. A separate possibility is that residues anywhere near 55 to 60 are especially sensitive to any type of change in the environment, considering the number of familial mutants that have been identified near there (H50Q, G51D, and A53T), our own identification of the significance of the T54S mutation, and the fact that the top interface in the Greek key structure spans some of those residues (shown in Figure 3.8). In any case, the chimeras provide further evidence that there is some interdependence between neighboring regions for the sequences of both asyn and bsyn.

Chapter 3.5 Threading the Sequence of Bsyn onto the Asyn Greek Key Fibril Structure Reveals Which Regions Would Be Especially Unstable in a Greek Key Conformation

After noticing that bsyn and chimeras containing the bsyn NAC were able to form fibrils at pH 5.8, we knew that the sequence of bsyn itself is not a barrier to fibril formation. Thus, we felt that trying to force bsyn's sequence into the same Greek key fibril structure of asyn should at least show why bsyn likely does not take on the same fibril structure and how flanking regions may influence the stability of the end fibrillar state. The set of structures shown reveal that due to gaps in the area of bsyn residues 44 to 97 where there are not many hydrophobic (Ala, Thr, Val, and Gly) residues, the Greek key structure would be greatly destabilized (Figure 3.8). Score per residue plots for the lowest scoring structure with constraints indicates that the C-terminal residues that are required to be present due to bsyn having a shorter NAC region are especially

destabilized, which leads to allosteric effects on the later bsyn NAC residues as well. The XAX chimeras do not deviate greatly in appearance from asyn from residues 30 to 97, and this is reflected in the especially close lowest total and per residue scores. The XBX chimeras have a wider distribution in the lowest total scores, but their high total scores indicate that none of these are likely to take on the Greek key conformation.

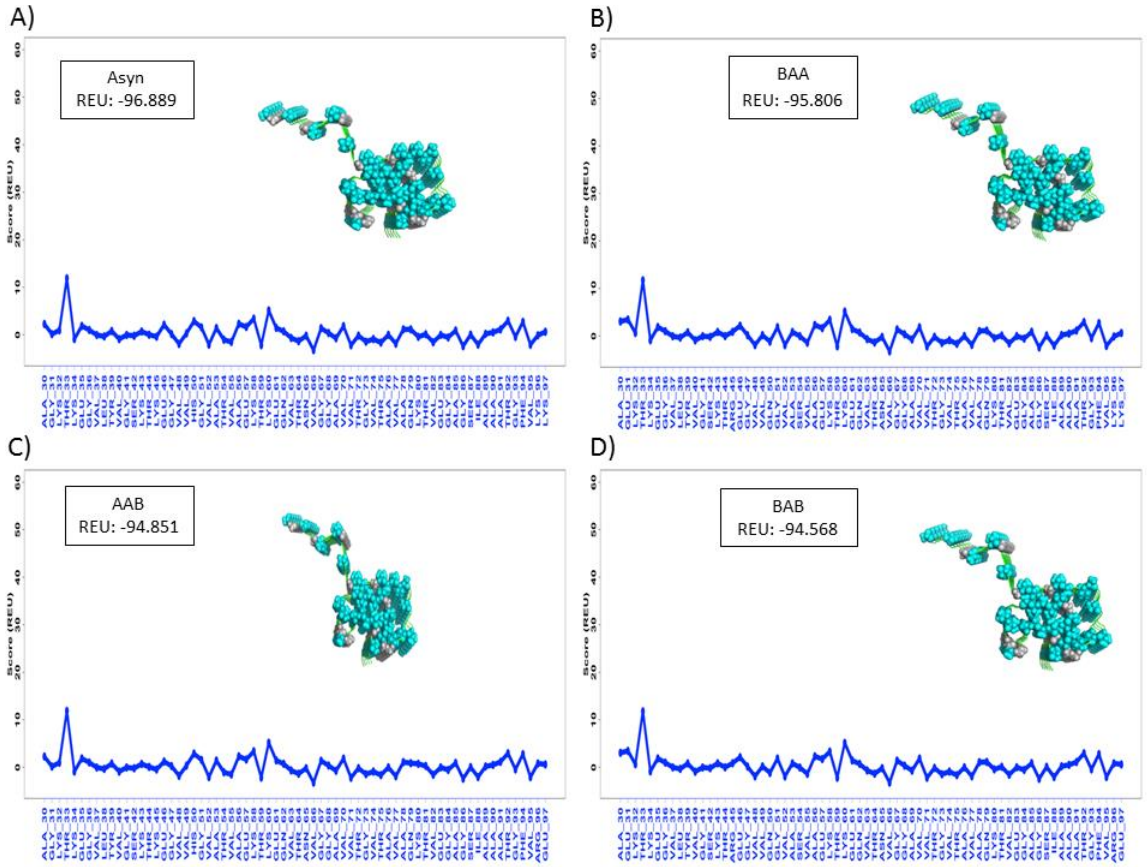

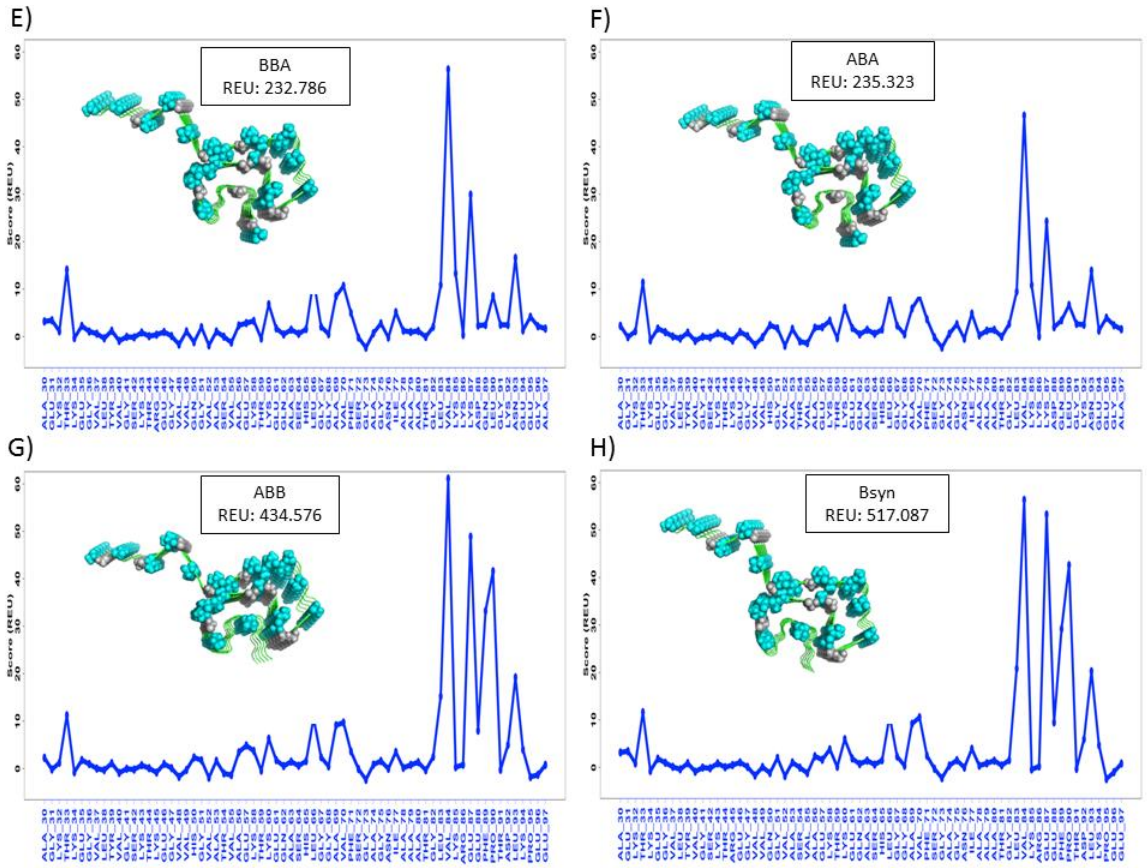

Figure 3.8. Lowest scoring asyn/XAX and bsyn/XBX chimera structures with constraints with corresponding per residue energy plots. Shown in A) through H) are plots of score in REU versus the corresponding residue (from residue 30 to 97) for the lowest scoring structure with constraints out of 1000 pdb files, with an inset showing an image of the lowest scoring structure along with the score in REU for the entire structure. A) through D) correspond to asyn and XAX chimeras, while E) through H) are bsyn and XBX chimeras. Note that in each structure, Ala, Val, and Thr residues are shown as blue spheres to indicate key hydrophobic patches, while Gly residues are shown as gray spheres, primarily to indicate turns. Higher total score indicates less stability for a given residue at that site.

One crucial feature in the Greek key structure of asyn is the GAG turn that effectively allows the lower portion of the fibril to fill in part of the hydrophobic core. It is possible for bsyn to have a turn at a GAG motif, but this occurs at residues 73-75 instead of 84-86 as it is in asyn. This may allow bsyn to keep the top interface, but the residues shown for the lower interface would likely be solvent exposed instead due to many of them being charged. A more likely possibility is that the bsyn residues from ~47 to 54 form an interface with some of the earlier N-terminal Ala, Val, and Thr residues that can be seen in each of the representative structures. The Greek key motif would not be present, but at least some portion of the hydrophobic contacts that are crucial to the fibril core could possibly be present when non-physiological conditions allow the protein to access alternate conformations. Bsyn could also have a lower number of conformations than asyn that would allow it to form a stable fibril, so the probability of a fibril forming is simply much lower than asyn and the non-physiological conditions greatly increase that probability.

Chapter 3.6 Allowing an Unconstrained Simulation Can Show How the Bsyn NAC May Compensate for Destabilization

The next logical step that our group considered was to try to determine what conformation bsyn's sequence may take on instead of forming the Greek key structure, given that we only had the ssNMR structure for asyn and knew how to substitute bsyn's and the chimeras' sequences into it. The two structures shown for bsyn and the XBX chimeras (Figure 3.9) mainly indicate that there simply is a wide distribution of possible conformations that the fibril could take on, while the single lowest scoring structure for

asyn and the XAX chimeras is likely to be an optimized conformation for each, given the much smaller distribution of rms values relative to the published asyn structure. A key feature worth noting is that in some of the lowest scoring XBX structures, the beta sheet region at the top of the structure (residues ~47 to 54) ended up being located underneath residues ~73 to 80, extending the hydrogen bonding for the beta sheets so that there were a total of 10 molecules in one continuous chain. This indicates that the interface between those two regions is destabilized to the point where hydrogen bonding interactions may start forming in place of the hydrophobic contacts that are present in asyn.

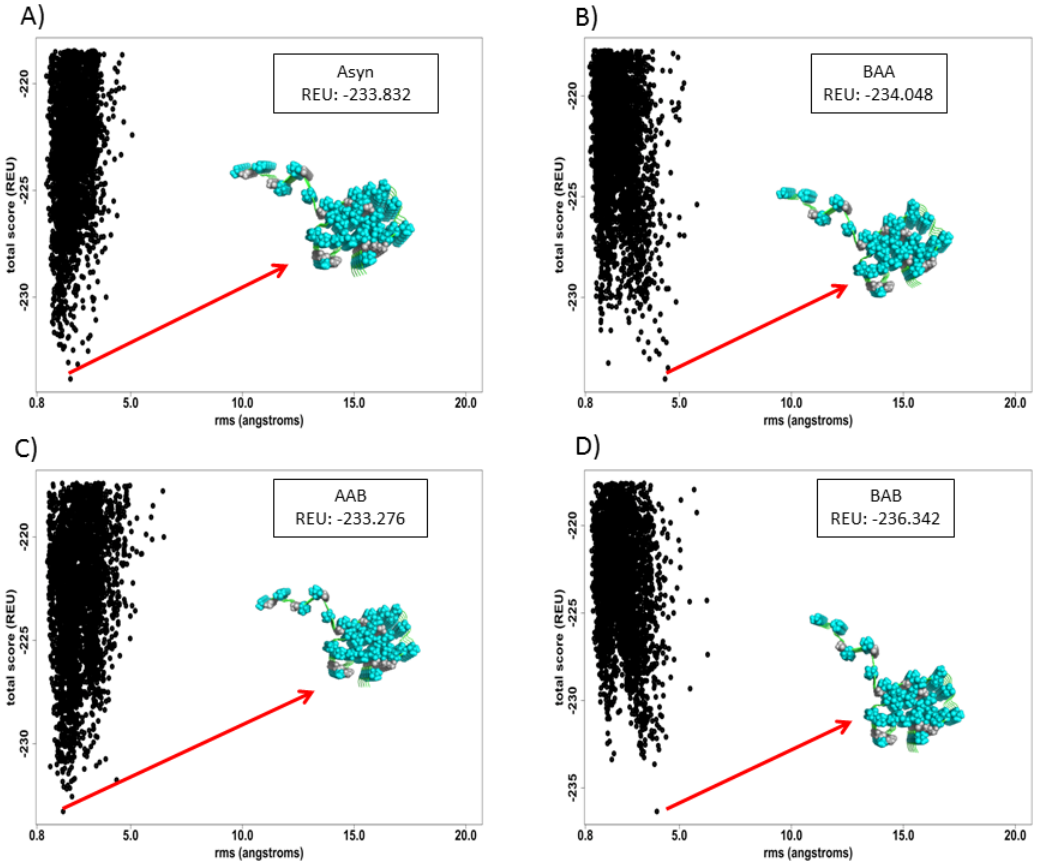

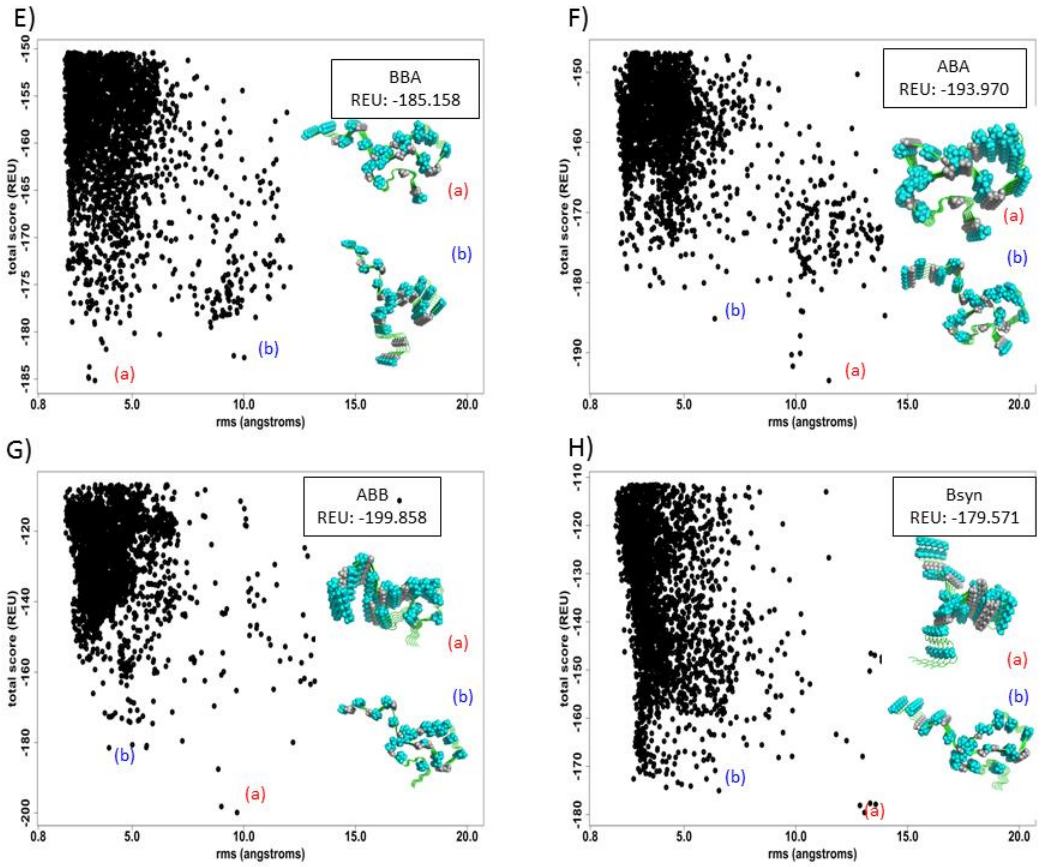

Figure 3.9. Rms versus score indicating distribution of structural changes in asyn/XAX and bsyn/XBX chimera structures without constraints. Plots of total score for each structure in REU versus rms relative to the starting published structure in angstroms are shown for asyn and XAX chimeras in A) through D), along with an image of the lowest scoring structure and the score in REU for that structure. The same type of plots are shown for bsyn and XBX chimeras in E) through G), with the lowest scoring structure shown as inset a) and another arbitrarily chosen low scoring structure shown as inset b). Note that these are the lowest 90% scoring structures in order to eliminate less plausible structures that resulted from Rosetta's FastRelax algorithm.

The hydrophobic residues indicated in the structures are especially significant because the Ala, Val, and Thr residues appear to interdigitate to some extent to form two key interfaces in asyn's structure, while Gly residues generally make the turns that allow the Greek key shape to exist. The lack of residues in bsyn's NAC means that the bottom interface would not actually be able to be formed, so a network of hydrophobic interactions can not be created. Instead, a network of hydrogen bonds along the fibril axis may be made, although the key result is that the top interface loses much of its stability due to the bottom interface not being present. This provides more evidence for the idea that bsyn recruits more N-terminal residues that may allow another interface to stabilize residues 47-54 that seem to be always present in the asyn NAC fibrils.

Chapter 4 Conclusions

By showing that certain combinations of domains lead to an increase in inhibition, more evidence has been provided that helps to explain how exactly bsyn is able to inhibit asyn aggregation, as well as giving a better sense of the exact effects that each of the individual domains of asyn have. The advantage of making every possible combination of domains is that two less predictable results were able to be obtained: the bsyn N-terminal region is probably less inhibiting than asyn's, and bsyn's NAC region is definitely a pH dependent switch for fibril formation of the full protein under non-physiological conditions. By supplementing these results with computational models of the asyn fibril, even more particular details were able to be proposed, such as the idea that while bsyn shares motifs like the GAG region that could allow for some kind of fibril formation, the high scores for other regions make clear that the fibrils are most likely not in a Greek key-like shape and need to overcome a significant energy barrier through some conformational changes induced by non-physiological conditions. Future studies could show how even more specific regions from bsyn's C-terminal domain could be used to inhibit asyn aggregation more effectively than the N-terminal peptides mentioned earlier, and other researchers could use the computational information perhaps to find a molecule that binds the asyn fibril in such a way that key regions are destabilized or possibly forced to take on a more bsyn-like conformation, perhaps through allosteric effects similar to the ones indicated here.

References

Allison, Jane R., et al. "A relationship between the transient structure in the monomeric state and the aggregation propensities of α-synuclein and β-synuclein." Biochemistry 53.46 (2014): 7170-7183.
Apetri, Mihaela M., et al. "Secondary structure of α-synuclein oligomers: characterization by raman and atomic force microscopy." Journal of molecular biology 355.1 (2006): 63-71.
Beyer, Katrin, et al. "Alpha-and beta-synuclein expression in Parkinson disease with and without dementia." Journal of the neurological sciences 310.1 (2011): 112-117.
Braga, Carolina A., et al. "The anti-Parkinsonian drug selegiline delays the nucleation phase of α-synuclein aggregation leading to the formation of nontoxic species." Journal of molecular biology 405.1 (2011): 254-273.
Chen, Li, et al. "Tyrosine and serine phosphorylation of α-synuclein have opposing effects on neurotoxicity and soluble oligomer formation." The Journal of clinical investigation 119.11 (2009): 3257-3265.
Cheruvara, Harish, et al. "Intracellular screening of a peptide library to derive a potent peptide inhibitor of α-Synuclein aggregation." Journal of Biological Chemistry 290.12 (2015): 7426-7435.
DiMaio, Frank, et al. "Modeling symmetric macromolecular structures in Rosetta3." PloS one 6.6 (2011): e20450.
EI-Agnaf, O. M. A., and G. B. Irvine. "Aggregation and neurotoxicity of α-synuclein and related peptides." Biochemical Society Transactions 30.4 (2002): 559-565.
Fares, Mohamed-Bilal, et al. "The novel Parkinson's disease linked mutation G51D attenuates in vitro aggregation and membrane binding of α-synuclein, and enhances its secretion and nuclear localization in cells." Human molecular genetics (2014): ddu165.
Fauvet, Bruno, et al. "α-Synuclein in central nervous system and from erythrocytes, mammalian cells, and Escherichia coli exists predominantly as disordered monomer." Journal of Biological Chemistry 287.19 (2012): 15345-15364.
Fusco, Giuliana, et al. "Direct observation of the three regions in α-synuclein that determine its membrane-bound behaviour." Nature communications 5 (2014).
Giasson, Benoit I., et al. "A hydrophobic stretch of 12 amino acid residues in the middle of α-synuclein is essential for filament assembly." Journal of Biological Chemistry 276.4 (2001): 2380-2386.
Gibson, D. "One-step enzymatic assembly of DNA molecules up to several hundred kilobases in size." Protocol Exchange (2009).
Hashimoto, Makoto, et al. "β-Synuclein inhibits α-synuclein aggregation: a possible role as an anti-parkinsonian factor." Neuron 32.2 (2001): 213-223.
Hong, Dong-Pyo, et al. "The role of the C-terminus of human α-synuclein: Intra-disulfide bonds between the C-terminus and other regions stabilize non-fibrillar monomeric isomers." FEBS letters 585.3 (2011): 561-566.
Irwin, David J., Virginia M-Y. Lee, and John Q. Trojanowski. "Parkinson's disease dementia: convergence of [alpha]-synuclein, tau and amyloid-[beta] pathologies." Nature Reviews Neuroscience 14.9 (2013): 626-636.

Janowska, Maria K., Kuen-Phon Wu, and Jean Baum. "Unveiling transient protein-protein interactions that modulate inhibition of alpha-synuclein aggregation by beta-synuclein, a pre-synaptic protein that co-localizes with alpha-synuclein." Scientific reports 5 (2015).
Jensen, Malene Ringkjøbing, Rob WH Ruigrok, and Martin Blackledge. "Describing intrinsically disordered proteins at atomic resolution by NMR." Current opinion in structural biology 23.3 (2013): 426-435.
Kang, Lijuan, et al. "The A53T mutation is key in defining the differences in the aggregation kinetics of human and mouse α-synuclein." Journal of the American Chemical Society 133.34 (2011): 13465-13470.
Kessler, Jeffrey C., Jean-Christophe Rochet, and Peter T. Lansbury. "The N-terminal repeat domain of α-synuclein inhibits β-sheet and amyloid fibril formation." Biochemistry 42.3 (2003): 672-678.
Khurana, Ritu, et al. "Mechanism of thioflavin T binding to amyloid fibrils." Journal of structural biology 151.3 (2005): 229-238.
Lavedan, Christian. "The synuclein family." Genome research 8.9 (1998): 871-880.
Lázaro, Diana F., et al. "Systematic comparison of the effects of alpha-synuclein mutations on its oligomerization and aggregation." PLoS Genet 10.11 (2014): e1004741.
Leaver-Fay, Andrew, et al. "ROSETTA3: an object-oriented software suite for the simulation and design of macromolecules." Methods in enzymology 487 (2011): 545.
Lemkau, Luisel R., et al. "Mutant protein A30P α-synuclein adopts wild-type fibril structure, despite slower fibrillation kinetics." Journal of Biological Chemistry 287.14 (2012): 11526-11532.
Lorenzen, Nikolai, and Daniel E. Otzen. "Oligomers of α-synuclein: picking the culprit in the line-up." Essays in biochemistry 56 (2014): 137-148.
Qin, Zhijie, et al. "Role of different regions of α-synuclein in the assembly of fibrils." Biochemistry 46.46 (2007): 13322-13330.
Rekas, Agata, et al. "The chaperone activity of α-synuclein: Utilizing deletion mutants to map its interaction with target proteins." Proteins: Structure, Function, and Bioinformatics 80.5 (2012): 1316-1325.
Rivers, Robert C., et al. "Molecular determinants of the aggregation behavior of α-and β-synuclein." Protein Science 17.5 (2008): 887-898.
Roodveldt, Cintia, et al. "A rationally designed six-residue swap generates comparability in the aggregation behavior of α-synuclein and β-synuclein." Biochemistry 51.44 (2012): 8771-8778.
Serpell, Louise C. "Alzheimer's amyloid fibrils: structure and assembly." Biochimica et Biophysica Acta (BBA)-Molecular Basis of Disease 1502.1 (2000): 16-30.
Shaltiel-Karyo, Ronit, et al. "Inhibiting α-synuclein oligomerization by stable cell-penetrating β-synuclein fragments recovers phenotype of Parkinson's disease model flies." PLoS One 5.11 (2010): e13863.
Sweers, Kim KM, et al. "Atomic force microscopy under controlled conditions reveals structure of C-terminal region of α-synuclein in amyloid fibrils." ACS nano 6.7 (2012): 5952-5960.
Tsigelny, Igor F., et al. "Dynamics of α-synuclein aggregation and inhibition of pore-like oligomer development by β-synuclein." Febs Journal 274.7 (2007): 1862-1877.
Tuttle, Marcus D., et al. "Solid-state NMR structure of a pathogenic fibril of full-length human [alpha]-synuclein." Nature structural & molecular biology (2016).

Uversky, Vladimir N. "Intrinsically disordered proteins and their environment: effects of strong denaturants, temperature, pH, counter ions, membranes, binding partners, osmolytes, and macromolecular crowding." The protein journal 28.7-8 (2009): 305-325.
Vilar, Marçal, et al. "The fold of α-synuclein fibrils." Proceedings of the National Academy of Sciences 105.25 (2008): 8637-8642.
Volpicelli-Daley, Laura A., et al. "Exogenous α-synuclein fibrils induce Lewy body pathology leading to synaptic dysfunction and neuron death." Neuron 72.1 (2011): 57-71.
Windisch, Manfred, et al. "β-synuclein-derived peptides with neuroprotective activity." Journal of Molecular Neuroscience 24.1 (2004): 155-165.
Winner, Beate, et al. "In vivo demonstration that α-synuclein oligomers are toxic." Proceedings of the National Academy of Sciences (2011): 201100976.
Wu, Kuen-Phon, et al. "Structural reorganization of α-synuclein at low pH observed by NMR and REMD simulations." Journal of molecular biology 391.4 (2009): 784-796.
Yamin, Ghiam, et al. "Forcing nonamyloidogenic β-synuclein to fibrillate." Biochemistry 44.25 (2005): 9096-9107.
Zibaee, Shahin, et al. "Sequence determinants for amyloid fibrillogenesis of human α-synuclein." Journal of molecular biology 374.2 (2007): 454-464.